Biomacromolecules

pubs.acs.org/Biomac

Article

Release Kinetics of Dexamethasone Phosphate from Porous Chitosan: Comparison of Aerogels and Cryogels

Coraline Chartier, Sytze Buwalda, Blessing C. Ilochonwu, Hélène Van Den Berghe, Audrey Bethry, Tina Vermonden, Martina Viola, Benjamin Nottelet, and Tatiana Budtova*

Cite This: *Biomacromolecules* 2023, 24, 4494–4501

Read Online

ACCESS | Metrics & More | Article Recommendations | Supporting Information

ABSTRACT: Porous chitosan materials as potential wound dressings were prepared via dissolution of chitosan, nonsolvent-induced phase separation in NaOH–water, formation of a hydrogel, and either freeze-drying or supercritical CO_2 drying, leading to "cryogels" and "aerogels", respectively. The hydrophilic drug dexamethasone sodium phosphate was loaded by impregnation of chitosan hydrogel, and the release from cryogel or aerogel was monitored at two pH values relevant for wound healing. The goal was to compare the drug-loading efficiency and release behavior from aerogels and cryogels as a function of the drying method, the materials' physicochemical properties (density, morphology), and the pH of the release medium. Cryogels exhibited a higher loading efficiency and a faster release in comparison with aerogels. A higher sample density and lower pH value of the release medium resulted in a more sustained release in the case of aerogels. In contrast, for cryogels, the density and pH of the release medium did not noticeably influence release kinetics. The Korsmeyer–Peppas model showed the best fit to describe the release from the porous chitosan materials into the different media.

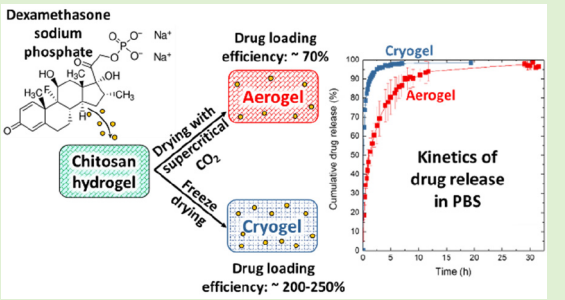

1. INTRODUCTION

Chitosan is a cationic polysaccharide produced via deacetylation of chitin, which in turn is obtained from crustacean shells. This seminatural polymer consists of D-glucosamine and *N*-acetyl-D-glucosamine units linked by β (1 → 4) glycosidic bonds. Chitosan has received considerable attention for use in biomedical applications owing to its biocompatibility as well as its antiviral, antifungal, and antibacterial properties.[1,2] For example, chitosan biomaterials have been extensively used as systems for the controlled delivery of biologically active agents.[3,4] Chitosan is of particular interest for the design of wound dressings due to unique features compared to most other dressing materials that have a passive role in wound healing. Chitosan has antimicrobial effects, it participates in the healing process through various mechanisms, including enhanced hemostasis and easier remodeling during the inflammatory and proliferative phases. The synergy of these properties and of specific drugs used for wound healing make chitosan carriers very promising materials.[5−7]

In general, drug release from a matrix depends on several material properties, such as matrix interactions with the drug, matrix solubility and swellability in the release medium, release medium composition (pH, ionic strength), and, if the matrix is porous, on its density, morphology, pore size distribution, and internal surface area. It is therefore important to establish processing–structure–property relationships, as they allow for the design of chitosan materials with tailored characteristics and the desired release behavior.

The delivery systems can be in a form of gels or dry matrices. If willing to make a dry porous material, solvent should be removed from a gel in a way that preserves network porosity. Different drying methods can lead to different material properties.[8,9] Here we do not consider membranes, which are a special class of porous materials. For example, evaporative drying from a gel, either *in vacuo* or at ambient pressure, usually leads to the collapse of pores due to capillary pressure resulting in materials with a high density and low porosity. Materials with a low density and high porosity can be obtained via supercritical (sc) drying (usually with sc CO_2 due to mild critical conditions), yielding "aerogels", or via freeze-drying, that are called "cryogels" for simplicity. In both drying methods, no meniscus is formed and, hence, capillary pressure is not relevant.

In the case of aerogels made from polysaccharides, the liquid in the precursor before drying should be miscible with CO_2, which is not the case for hydrogels. Water is thus replaced by

Special Issue: Polymers for Unmet Medical Challenges: Papers Presented at the Advanced Functional Polymers Medicine 2022 Conference

Received: November 25, 2022
Revised: February 20, 2023
Published: March 23, 2023

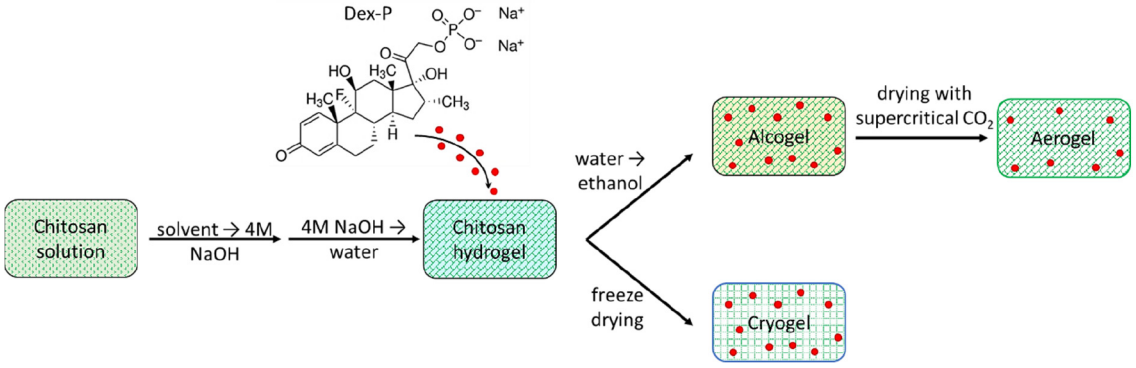

Figure 1. Schematic representation of the preparation process of Dex-P loaded-chitosan cryogels and aerogels.

ethanol or acetone, which are usually nonsolvents for natural polysaccharides, as well as CO_2. Depending on the polymer molecular weight, chain rigidity, and interaction parameters, the material is shrinking, but the network morphology may still be reasonably well preserved, resulting in materials with high porosity, above 90%, and a high specific surface area of several hundreds of m^2/g.[10] In contrast, for cryogels, if water is in the pores of the network, the growth of ice crystals during freezing can generate large pores and channels with sizes from several micrometers to several tens of micrometers. These materials generally display a lower internal surface area in comparison with aerogels. Of notice, the morphology of aerogels and cryogels can be very different even at the same material density.[8,9,11] Other ways of making porous chitosan, such as using surfactants,[12] making bubbles by sonication,[13] or leaching out a sacrificial substance,[14] usually do not result in materials with low density and high specific surface area.

Several papers reported on the use of chitosan-based aerogels and cryogels as controlled drug delivery systems. For example, chitosan-collagen cryogels coated with poly(*N*,*N*′-diethylacrylamide) were developed for temperature- and pH-responsive delivery of the anti-inflammatory drug ibuprofen.[15] Furthermore, chitosan-alginate aerogel microparticles were developed for pulmonary delivery of the anticancer drug cisplatin.[16] The field of porous chitosan-based materials for drug delivery purposes was extensively reviewed in two recent publications.[17,18] In all papers related to porous chitosan-based drug delivery systems, only one drying method was employed on studied chitosan solutions and gels, which makes it complicated to develop correlations between the drying technique, the structural and morphological properties of the material, and its release behavior.

Previously, we described the influence of drying conditions (sc drying versus freeze-drying) on the physicochemical properties of non-cross-linked chitosan porous materials.[19] In the current manuscript, we investigate the release kinetics of the hydrophilic drug dexamethasone sodium phosphate, a synthetic corticosteroid with anti-inflammatory effects, from chitosan aerogels and cryogels prepared from the same precursor (i.e., chitosan hydrogel). The drug-loading efficiency and release kinetics are discussed with respect to the processing conditions, the network morphology of the materials, their physicochemical properties, and the pH of the release medium. The Korsemeyer–Peppas equation is used to identify the dominant physical mechanism controlling the release.

2. MATERIALS AND METHODS

2.1. Materials. Chitosan of molecular weight 691000 g/mol and degree of acetylation 7%[19] was purchased from Acros. Glacial acetic acid, ethanol (purity higher than 99%), and sodium hydroxide pellets (analytical reagent grade) were supplied by Fisher Chemical. Dexamethasone sodium phosphate (Dex-P) was supplied by Sigma. Phosphate buffer saline (PBS) 10× solution was acquired from Fisher bioreagents (Pittsburgh, PA, U.S.A.). All chemicals were used as received. Water was distilled.

2.2. Methods. *2.2.1. Preparation of Chitosan Aerogels and Cryogels.* Chitosan aerogels and cryogels were prepared as described elsewhere.[19] Briefly, chitosan was dissolved in 2%v/v acetic acid under mechanical stirring at room temperature. The concentration of chitosan was 5 or 8% wt/v. Approximately 6 mL of chitosan solution was poured into polypropylene molds (27.5 mm in diameter with holes in the walls of about 1 mm in diameter spaced 2–4 mm apart; the holes were made for the subsequent homogeneous solvent to nonsolvent exchange). The molds were immersed for 24 h in 100 mL of 4 M NaOH–water solution for nonsolvent-induced phase separation. As demonstrated in our previous work, this NaOH concentration allowed obtaining stable-in-shape samples; no influence of NaOH concentration above 1 M on aerogels' and cryogels' properties was reported.[19]

The obtained samples were gently demolded, and NaOH was removed with consecutive water baths, resulting in "hydrogels" (Figure 1). The hydrogels (approximately 5 mL in volume) were subsequently loaded with the drug by immersing in 100 mL of 0.5 g/L Dex-P aqueous solution for 3 days under magnetic stirring at 100 rpm.

To obtain "aerogels", drying was performed with sc CO_2. As water is not miscible with CO_2, water in the hydrogels was replaced by ethanol by adding ethanol to the hydrogel with ethanol to hydrogel volume ratio around 24/1. No gradual solvent exchange was performed as described previously[19] to prevent, as much as possible, washing out of the drug (Dex-P is poorly soluble in ethanol and in ethanol–water mixtures[20]). To ensure complete removal of water, ethanol was renewed twice a day for 2 days, resulting in "alcogels" (Figure 1). Drying with sc CO_2 was performed as described elsewhere.[21,22] The system was pressurized at 50 bar and 37 °C, and ethanol was slowly washed with gaseous CO_2. Afterward, the pressure in the autoclave was increased to 80 bar to be above the CO_2 critical point. The sc CO_2 solubilized the residual ethanol inside the sample pores. A washing step was performed at 37 °C with an output of 5 kg of CO_2/h for 1 h. It was followed by a static (recirculation) step of 1–2 h in the same conditions followed by a washing step again for 2 h. The system was then depressurized at 4 bar/h and cooled to room temperature before opening the autoclave.

To obtain "cryogels", the hydrogels were immersed in liquid nitrogen (−196 °C) for 5 min and placed in a freeze-dryer (Cryotec Cosmos 80) for lyophilization for 48 h.

2.2.2. Characterization of Chitosan Cryogels and Aerogels. The bulk (or apparent) density ρ_{bulk} of chitosan aerogels and cryogels was obtained by measuring sample dimensions with a caliper and weight with a high-precision balance. The porosity was calculated from the

https://doi.org/10.1021/acs.biomac.2c01408
Biomacromolecules 2023, 24, 4494–4501

Table 1. Bulk Density, Specific Surface Area, Drug-Loading Efficiency (DLE), and Drug-Loading Capacity (DLC) for Aerogels and Cryogels

type of sample	chitosan concentration in solution, %wt/v	density, g/cm^3	specific surface area, m^2/g	DLE, %	DLC, %
aerogel	5	0.064 ± 0.005	261 ± 34	67 ± 2	0.53 ± 0.04
	8	0.124 ± 0.006	245 ± 1.1	68 ± 6	0.28 ± 0.03
cryogel	5	0.058 ± 0.004	48 ± 4	252 ± 58	2.2 ± 0.45
	8	0.098 ± 0.017	51 ± 4	206 ± 27	1.05 ± 0.07

bulk and skeletal (or true) density ($\rho_{skeletal}$, 1.446 ± 0.116 g/cm^3)[7] with eq 1:

$$\text{porosity}(\%) = (\rho_{skeletal} - \rho_{bulk}) \times 100/\rho_{skeletal} \quad (1)$$

The specific surface area was measured using ASAP 2020 (Micromeritics) employing the Brunauer, Emmett et Teller (BET) approach. Prior to measurements, the samples were degassed in a high vacuum at 70 °C for 10 h.

The morphology of the samples was studied with a Scanning Electron Microscope (SEM) MAIA (Tescan) equipped with a field emission gun at an accelerating voltage of 3 keV. To avoid the accumulation of electrostatic charges and images' defaults, a layer of platinum (14 nm) was applied on the samples using a Q150T Quarum rotating metallizer.

Sample volume evolution ΔV during drug release was determined from sample volume before (V_i) and after (V_f) the release, each obtained by measuring disk-shaped samples' diameter and height:

$$\Delta V(\%) = (V_f - V_i) \times 100/V_i \quad (2)$$

2.2.3. Drug Release. First, the calibration curve to be used for the determination of Dex-P concentration in the release bath, PBS, at pH 7.4 and 8.9, was established using an Acquity ultra high-performance liquid chromatography system (Waters Corporation, Milford, U.S.A.) operated by Empower software (Version 3-FRS, Waters Corporation). A BEH C18 column was used at 50 °C. The injection volume was 10 μL, with 25%ACN/75% Milli-Q water as eluent, acidified with 0.1% perchloric acid to yield pH 2.2. The run time was 5 min, the retention time 0.6 min and the flow rate 1 mL/min. The detection wavelength was 254 nm. The peak area was plotted as a function of the known Dex-P concentration in the interval 1−100 μg/mL (Figure S1).

Drug release kinetics was monitored under sink conditions in 150 mL of PBS under magnetic stirring at 100 rpm at 30 °C (temperature of skin) and at pH 7.4 or 8.9. These two values were selected as the pH of a chronic wound decreases from 8.9 (inflammation stage) to 7.2 (healing stage).[23−25] The chitosan sample (diameter around 22 mm, height around 11 mm and weight between 0.26 and 0.58 g depending on the initial chitosan concentration) was placed in a tea-bag and immersed in the PBS release medium. Release medium (1 mL) was taken out regularly and replaced by an equal amount of fresh medium; the dilution was taken into account when calculating the Dex-P concentration. The Dex-P release was monitored until no evolution of drug concentration occurred for several hours. Then, the sample was crushed with a mortar and pestle and dispersed in 20 mL PBS solution. The dispersion was sonicated for 30 min to ensure a complete release of the drug from the sample, if any, filtered through a 0.22 μm cellulose acetate filter and the Dex-P concentration was determined using the calibration curve. As no drug was detected in the release bath, we deduce that no drug remained in the chitosan matrix within experimental error. The Dex-P concentration in the matrix before release was thus considered to be the one obtained after complete release. All measurements were performed in duplicate.

The drug-loading efficiency (DLE) and the drug-loading capacity (DLC) were calculated as follows:

$$\text{DLE}(\%) = \frac{\text{actual drug dose(g)}}{\text{theoretical drug dose(g)}} \times 100 \quad (3)$$

$$\text{DLC}(\%) = \frac{\text{actual drug dose(g)}}{\text{chitosan matrix mass(g)}} \times 100 \quad (4)$$

where the actual drug dose is the mass of Dex-P in the chitosan matrix and theoretical drug dose corresponds to the drug dose in the chitosan sample after the drug loading process (Figure 1) assuming only diffusion-driven equal distribution of Dex-P within the sample and the loading bath. As the volume of hydrogel was much smaller than that of the loading bath (5 vs 100 mL), and no swelling or contraction of hydrogel was recorded, the theoretical drug concentration after loading is slightly lower (0.48 g/L) in comparison with in the initial bath (0.5 g/L).

2.2.4. Cytotoxicity Study. The cytotoxicity study was performed in compliance with ISO 10993 guideline, parts 5 and 12, following the extract method. Prior to extraction, aerogels were decontaminated by irradiation at 254 nm for 5 min. Then complete cell culture medium (DMEM 4, 5 g/L D-glucose supplemented with 5% FBS (10% FBS for HDF cells), 1 mM L-glutamine, 100 units/mL penicillin, and 100 μg/mL streptomycin) was added to achieve an extraction ratio of 0.1 g/mL. Extraction was done for 24 h at 37 °C under stirring.

The same extraction ratio was used to prepare standard reference biomaterials: negative control material RM-C (high density Polyethylene batch C-141) and positive control RM-A (0.1% zinc diethyldithiocarbamate polyurethane film batch A-202 K) purchased from Hatano Research Institute, Food and Drug Safety Center, Japan.

Murine fibroblasts L929 (ECACC 85011425) and Human Dermal Fibroblasts (HDF) P3 (Gibco C-013-5C) fibroblasts were seeded at 1.104 cells per well (96-well plate) and allowed to adhere overnight. Then, 100% extracts were added to L929 and NHDF cell monolayers. Cell viability was assessed after 24h incubation at 37 °C under humidified atmosphere with 5% CO_2 with the CellTiter Glo assay (Promega G7571) according to the manufacturer's instructions.

2.2.5. Statistics. Data are expressed as means ± SD and correspond to measurements with $N = 2$ for drug release studies and $N = 3$ for all other experiments.

3. RESULTS AND DISCUSSION

3.1. Influence of Aero- and Cryogel Properties on Drug-Loading Efficiency and Drug-Loading Capacity. Two parameters were varied during sample preparation: the chitosan concentration (5 or 8 wt %/v) and the drying method (freeze-drying or supercritical drying with CO_2). The influence of these parameters on material density, porosity, and specific surface area have been extensively described in our previous work.[19] Briefly, when a nonsolvent (here, 4 M NaOH−water) is added to chitosan solution, a nonsolvent-induced phase separation occurs, resulting in a 3D chitosan network with NaOH−water in the pores. A similar approach is known for the fabrication of cellulose aerogels.[26] The advantage of this process is the absence of any cross-linker, which can induce adverse effects in biomedical applications. A higher chitosan concentration resulted in aerogels with a higher density and lower porosity; the surface area was not substantially influenced. Aerogels were of slightly higher density and with significantly higher surface area as compared to their cryogel counterparts. Higher density of chitosan aerogels as compared to cryogels is due to "cumulated" shrinkage (within 30 vol %)

https://doi.org/10.1021/acs.biomac.2c01408
Biomacromolecules 2023, 24, 4494−4501

occurring at each processing step, from solution to hydrogel then to alcogel and finally to aerogel. In the preparation of cryogels, shrinkage is negligible, as there is no step of hydrogel immersion in ethanol and in CO_2, both being nonsolvents of chitosan.

Drug-loading efficiency (DLE, eq 3), together with aerogel and cryogel characteristics, is shown in Table 1, and examples of materials' morphology are shown in Figure 2. DLE of

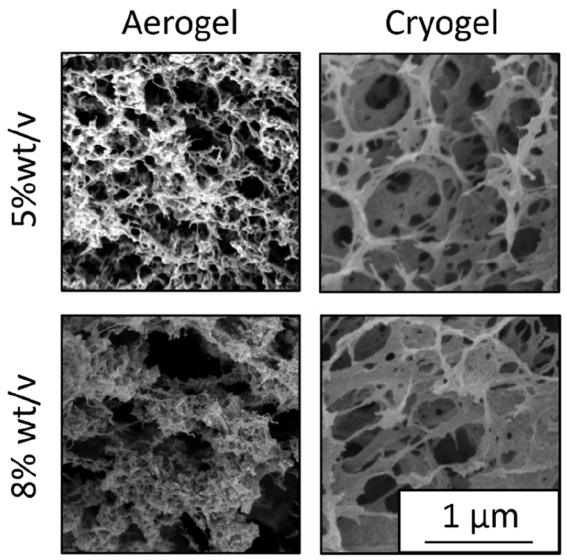

Figure 2. SEM images of chitosan cryogels and aerogels made from 5 and 8% wt/v solutions, the scale is the same for all images. Their corresponding characteristics are given in Table 1.

aerogels is lower than those of cryogels, around 70% vs 200−250%, respectively. For aerogels, the reason is that, despite the poor solubility of Dex-P in ethanol and in water/ethanol mixtures with a high ethanol content,[20] the drug was most probably partly washed out during water to ethanol exchange. Some washing out could have also occurred during supercritical drying. A similar phenomenon was observed for pectin aerogels loaded with theophylline.[9] Neither density nor surface area of aerogels or cryogels had a marked influence on the loading efficiency within the intervals studied, but the latter are too narrow to deduce trends. Nevertheless, 70% loading efficiency in aerogels is relatively high compared to other bioaerogels reported in the literature for other various drugs: 13−23% for alginate-based aerogels,[27] 16−80% for pectin-based aerogels,[27,28] 15−27% for starch-based aerogels,[27] and 50−100% for cellulose−pectin aerogels.[29]

Interestingly, the loading efficiency of the cryogels is much above 100% which means that the drug is adsorbed by the chitosan during immersion of the hydrogel in the drug solution. This is due to the ionic interactions between positively charged amino groups of chitosan (the pK_a of chitosan is around 6.3−6.4[30]) and the negatively charged phosphate group of Dex-P, as demonstrated previously.[31,32]

Drug-loading capacity (DLC, eq 4) follows the same trends as DLE (Table 1), as expected. It is around 0.25−0.50% for aerogels and 1.7−2.8% for cryogels. A higher chitosan concentration results in a lower DLC due to a higher chitosan matrix mass. The obtained DLC is lower than that for other bioaerogels, for example, aerogels based on pectin (2−37%),[27,28,33] alginate (12−21%),[27,34] starch (10−25%),[27,34] or cellulose−pectin (2−4%)[29] due to the relatively low Dex-P concentration in the loading bath and relatively high concentrations of chitosan. However, the obtained loading capacity of aerogels, and especially of cryogels, is much higher than that (0.14%) of freeze-dried chitosan impregnated with dexamethasone using supercritical fluid technology.[35]

3.2. Kinetics of Dexamethasone Sodium Phosphate Release from Chitosan Aerogels and Cryogels. The Dex-P cumulative release kinetics from chitosan aerogels and cryogels of different densities is illustrated in Figure 3a and b, respectively, and the comparison of the drug release from aerogel and cryogel of the same density is shown in Figure 3c. The same data as in Figure 3c but in absolute (non-normalized) scale are shown in Figure S3. The higher is the density of the aerogel, the slower is the release, as expected,[28] as drug diffusion is hindered by a denser network. However, density does not influence the release kinetics from chitosan cryogels in the interval studied which may be the consequence of the very large macropores present in the cryogels. The larger the pore dimensions, the weaker is the influence of density provided the materials still remain highly porous and loading is the same. The influence of morphology on release kinetics is clearly visible in Figure 3c for aerogels and cryogels of the same density: the release is much faster from cryogels. At least two reasons can be at the origin of this fast release: one is higher drug concentration in the matrix (see Table 1 and also Figure S3) and the other is larger pores (and thus lower tortuosity) in

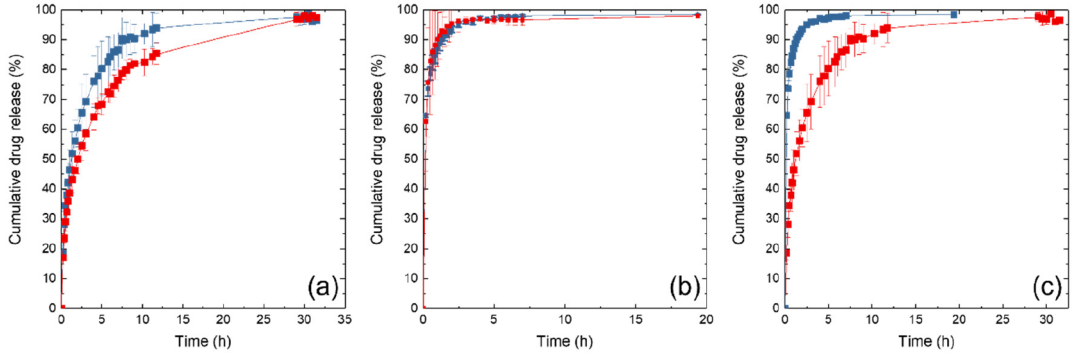

Figure 3. Kinetics of Dex-P release in PBS at pH 7.4 and 30 °C from (a) chitosan aerogels of density 0.06 g/cm^3 (blue) and 0.11 g/cm^3 (red); (b) chitosan cryogels of density 0.06 g/cm^3 (blue) and 0.09 g/cm^3 (red) and (c) from aerogel (red) and cryogel (blue), both of the same density 0.06 g/cm^3. Lines are given to guide the eye.

https://doi.org/10.1021/acs.biomac.2c01408
Biomacromolecules 2023, 24, 4494−4501

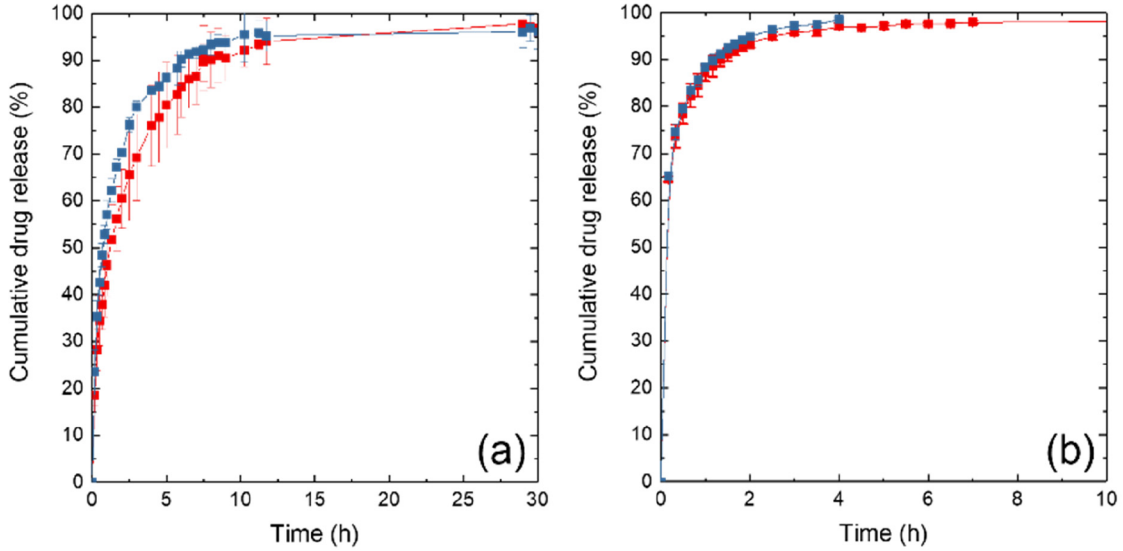

Figure 4. Cumulative drug release into PBS at 30 °C as a function of time at pH 7.4 (red) and 8.9 (blue) from (a) chitosan aerogels (density 0.06 g/cm^3) and (b) chitosan cryogels (density 0.06 g/cm^3). Lines are given to guide the eye. If the error bars are not visible, they are smaller than or equal to the size of symbols.

comparison with aerogels. The latter is shown in Figure 2 and also demonstrated in our previous work.[19]

The influence of the pH of the release medium, 7.4 vs 8.9, on Dex-P release kinetics is illustrated in Figure 4a and b. The release from aerogels is slightly faster at pH 8.9 as compared to pH 7.4 (Figure 4a): for example, 80% of cumulative release from aerogels of density 0.06 g/cm^3 occurs in 3 h at pH 8.9 vs 5 h at pH 7.4. As mentioned above, due to the ionic interactions between amino groups of chitosan and the phosphate group of Dex-P, the drug is likely to be bound to the polymer. We hypothesize that higher is pH of the release medium, faster is Dex-P decomplexation from chitosan and thus faster the release. In contrast, the pH of the release medium practically does not influence the kinetics of Dex-P release from cryogels (Figure 4b). Although the same mechanism also occurs in cryogels, its effect on the Dex-P release is not noticeable because of the fast release caused by the large macropores, as in the case shown above in Figure 3b, making cryogels a less "sensitive" matrix. This difference in pH sensitivity between cryogels and aerogels may be exploited for wound healing as for the later, a faster release would be encountered during the inflammation step (pH 8.9) and a slower one once entering the healing stage (pH 7.4).

Figure S3 shows the concentration of Dex-P in the release medium as a function of time for aerogels and cryogels, both of the same density. The ideal Dex-P dose and kinetics of release depend on the wounded tissue and the desired therapeutic effect. For example, a Dex-P concentration of ~400−600 μg/mL was reported for cellulose based wound dressing.[36] These dressings were effective in preventing wound fibrosis. In another study, it was shown that a much lower concentration (0.5−3.5 μg/mL), obtained with Dex-P releasing from cellulose/agar tablets, is effective to trigger buccal wound healing.[37] The concentrations of Dex-P in aerogels and cryogels obtained in our work (some tens of μg/mL, see Figure S3) are in between the values presented in the publications cited above; by modulating the type of material (cryogel or aerogel), its density, and the drug concentration in the loading bath, drug concentration in our porous chitosans can be adjusted to the desired therapeutic response.

3.3. Selection of a Kinetic Model to Describe the Release of Dex-P from Chitosan Aerogels and Cryogels.

As for the majority of drug delivery systems, the release from aerogels and cryogels can be divided into two phases (Figures 3 and 4): a first one representing fast release and a second one in which the curve levels off toward end of release of the drug from the matrix. The duration of the first phase (50−60% of cumulative release) is from 1 to 3 h for aerogels and is very fast, within 10 min, for cryogels. On one hand, such highly fast drug release, similar to burst release, may be a drawback for wound dressing applications as it may lead to toxic effects due to the high concentration reached in the surrounding tissues. A too fast release can also be considered as an economical waste, as the treatment would require a more frequent drug administration and thus replacement of the dressing.[38] On the other hand, a fast release may help reaching an effective concentration quickly, e.g., for a pain-killing drug.

It should be noted that when drug-loaded chitosan materials were immersed in the release medium, the samples were shrinking, and this occurred during the first few minutes after immersion. No dissolution of the matrix was observed, as expected in view of the insolubility of chitosan at these pH values. A sharp volume decrease can be one of the reasons for the fast increase of drug concentration in the release medium. Aerogels are shrinking more than cryogels, with ΔV (see eq 2) being around 50−60% vs 20−40%, respectively (see Figure S2). The shrinkage is due to the capillary pressure occurring when a porous material is immersed in a liquid. Capillary pressure is defined by the Young−Laplace equation which predicts higher pressure, and thus enhanced pore collapse, for smaller pores. The difference in pore size explains why aerogels are shrinking more than cryogels.

Various mathematical models are used to describe release kinetics from a solid polymer matrix.[39] Since 60% of cumulated release from cryogels was reached very quickly, there were not sufficient data points for the modeling of the release kinetics. Zero-order model is not applicable to approximate the release

https://doi.org/10.1021/acs.biomac.2c01408
Biomacromolecules 2023, 24, 4494−4501

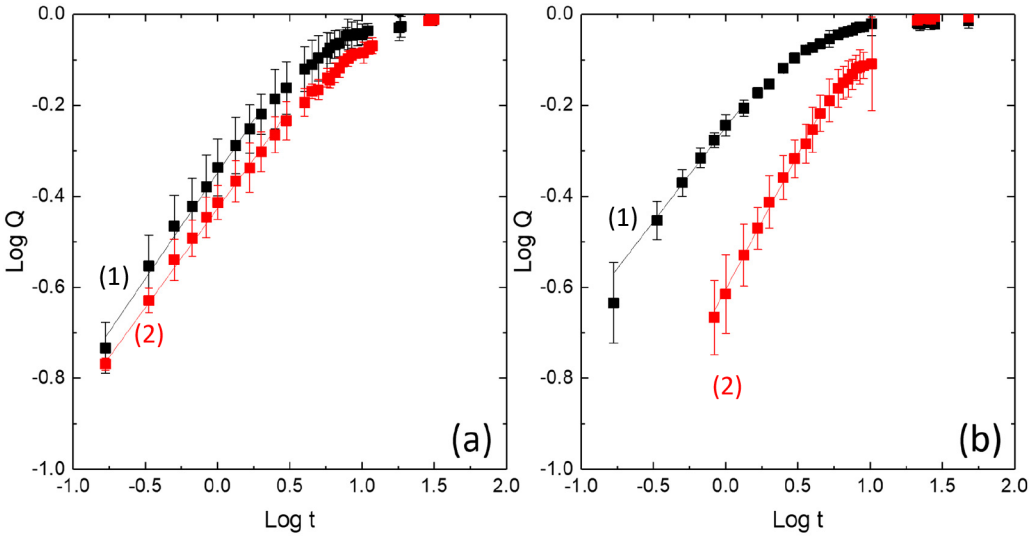

Figure 5. Fit of experimental data by the Korsmeyer–Peppas model (solid lines) for Dex-P release into the bath of pH 7.4 (a) and 8.9 (b) from aerogels of density 0.064 (1) and 0.124 (2) g/cm^3.

from aerogels as the slope of cumulative release varies during the release. As chitosan aerogels are not swelling or dissolving in PBS, all models that consider polymer relaxation and/or erosion should not be considered, nor should be the Ritger–Korsmeyer–Peppas model which predicts burst release. The Higuchi model is not applicable either as the main requirement, i.e., the initial drug concentration in the system to be higher than drug solubility, is not fulfilled. Thus, two models that may describe the first 60% of release were tested to fit experimental data of Dex-P release kinetics from chitosan aerogels: first-order kinetics and the Korsmeyer–Peppas approach.

The first-order kinetic model predicts the following dependence of the cumulated release Q as a function of release time t:

$$\log(1 - Q) \sim A \times t \tag{5}$$

where A is a constant. For first-order release, the drug release rate is directly proportional to the concentration gradient and is a function of the amount of drug remaining in the matrix. An example in Figure S4 shows that the fit of this model to experimental data is not good, and thus, it will not be used. We hypothesize that one of the reasons is the ionic interactions between Dex-P and chitosan. Finally, the Korsmeyer–Peppas approach was applied to the first 60% of the cumulated release:

$$Q \sim K \times t^n \tag{6}$$

where K and n are constants. According to our experimental setup (see Methods), the sample can be approximated by a cylinder. The results are shown in Figure 5a,b and in Table 2, demonstrating that the Korsmeyer–Peppas approach provides the best fit to experimental data with the correlation coefficient R^2 = 0.99. In most cases the exponent n is around 0.45, corresponding to Fickian diffusion, as expected.[39−41] However, the exponent describing the release kinetics in the bath at pH 8.9 is higher than 0.45, which theoretically should correspond to anomalous transport. As no matrix swelling or dissolution was observed, we hypothesize that this unexpected result is due to accelerated decomplexation of Dex-P molecules from chitosan chains, as the amine groups on chitosan are less protonated at higher pH and therefore have less interaction with negatively charged Dex-P.

Table 2. Korsmeyer–Peppas Fitting Constants (Eq 6) for the Kinetics of Dex-P Release from Chitosan Aerogels into Release Media of Different pH Values

	pH of release medium: 7.4			pH of release medium: 8.9		
chitosan aerogel density, g/cm^3	n	K	R^2	n	K	R^2
0.064	0.47	0.46	0.99	0.47	0.57	0.99
0.124	0.42	0.38	0.996	0.59	0.24	0.99

3.4. Cytotoxicity Assays. The cytotoxicity of the chitosan aerogels prepared from 5% wt/v chitosan solutions was finally assessed (Figure 6). Considering the targeted wound dressing application, two fibroblasts cell lines were chosen: L929 murine fibroblasts were selected with respect to the ISO 10993 guidelines and Human Dermal Fibroblasts (HDF) were selected to assess the aerogels with human cell lines. The extracts from chitosan aerogels, negative control material RM-C or positive control RM-A were added on fibroblasts seeded into the well, and cell viability was evaluated over a 24 h period. Only extracts from positive control films (RM-A) showed low cell viability for both cell types. The extracts from chitosan aerogels induced viability above 70% as compared with TCPS control (Figure 6) for both types of fibroblasts and values were similar to the negative control material RM-C. These results demonstrate the absence of cytotoxicity of chitosan aerogels toward fibroblasts and confirm their potential use for wound dressings.

4. CONCLUSIONS

The release of dexamethasone-phosphate from porous chitosan materials, aerogels, and cryogels was investigated in two buffer solutions: one at pH 7.4, approximating the pH value of a chronic wound in the healing stage, and one at pH 8.9, corresponding to the pH value of a chronic wound in the inflammation stage. Drug-loading efficiency in cryogels was three times higher than in aerogels and exceeded 200%. This interesting result is due to the ionic interactions between positively charged amino groups of chitosan and the negatively

https://doi.org/10.1021/acs.biomac.2c01408
Biomacromolecules 2023, 24, 4494−4501

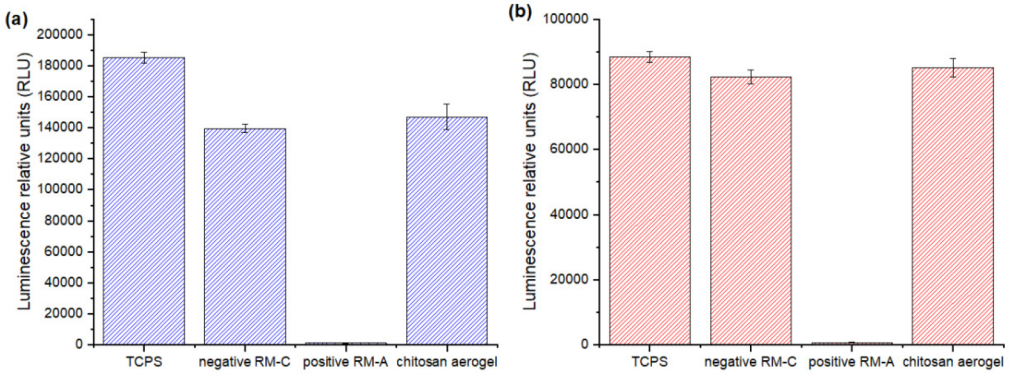

Figure 6. Cell viability evaluation assessed on (a) murine fibroblast L929 cells and (b) human dermal fibroblasts (HDF) after 24 h exposition with 100% extracts of reference materials (RM-C and RM-A) or 100% chitosan extract.

charged phosphate group of dexamethasone phosphate. Drug-loading efficiency in aerogels is high, around 70%, but it is lower than 100%, likely due to two factors: potential solubility of the drug in the water−ethanol mixture during the first step of solvent exchange, and "mechanical" washing-out during supercritical drying.

The release from chitosan aerogels and cryogels was shown to depend on material density and morphology. Slower release was recorded from aerogels of higher density, as expected; whereas cryogel density did not influence the release kinetics within the interval studied. At the same material density, the release of Dex-P from cryogels was faster than from aerogels, which was ascribed to the different material morphologies: large pores and channels in cryogels vs smaller pores with high tortuosity in aerogels. We hypothesize that aerogels exhibit a faster release at pH 8.9 than at pH 7.4 due to decreased ionic interactions between chitosan and Dex-P. The Korsmeyer−Peppas model showed the best fit to experimental data. Chitosan aerogels were noncytotoxic toward HDF and L929 cells.

Overall, it was demonstrated that Dex-P loaded chitosan porous materials can be made with various porosity and morphology, which results in different release kinetics making these materials promising for biomedical applications.

■ ASSOCIATED CONTENT

Supporting Information

The Supporting Information is available free of charge at https://pubs.acs.org/doi/10.1021/acs.biomac.2c01408.

(1) Calibration curves for Dex-P dissolved in PBS; (2) Volume shrinkage of chitosan aerogels and cryogels in PBS; (3) Concentration of Dex-P in the release medium as a function of time for aerogels and cryogels; (4) Fit of experimental data by the first order model for Dex-P release (PDF)

■ AUTHOR INFORMATION

Corresponding Author

Tatiana Budtova − *MINES Paris, PSL University, Center for Materials Forming (CEMEF), 06904 Sophia Antipolis, France;* orcid.org/0000-0003-1835-2146; Email: tatiana.budtova@minesparis.psl.eu

Authors

Coraline Chartier − *MINES Paris, PSL University, Center for Materials Forming (CEMEF), 06904 Sophia Antipolis, France; Department of Polymers for Health and Biomaterials, IBMM, Univ. Montpellier, CNRS, ENSCM, 34090 Montpellier, France*

Sytze Buwalda − *MINES Paris, PSL University, Center for Materials Forming (CEMEF), 06904 Sophia Antipolis, France*

Blessing C. Ilochonwu − *Division of Pharmaceutics, Utrecht Institute for Pharmaceutical Sciences (UIPS), Utrecht University, Utrecht 3508 TB, The Netherlands*

Hélène Van Den Berghe − *Department of Polymers for Health and Biomaterials, IBMM, Univ. Montpellier, CNRS, ENSCM, 34090 Montpellier, France*

Audrey Bethry − *Department of Polymers for Health and Biomaterials, IBMM, Univ. Montpellier, CNRS, ENSCM, 34090 Montpellier, France*

Tina Vermonden − *Division of Pharmaceutics, Utrecht Institute for Pharmaceutical Sciences (UIPS), Utrecht University, Utrecht 3508 TB, The Netherlands;* orcid.org/0000-0002-6047-5900

Martina Viola − *Division of Pharmaceutics, Utrecht Institute for Pharmaceutical Sciences (UIPS), Utrecht University, Utrecht 3508 TB, The Netherlands*

Benjamin Nottelet − *Department of Polymers for Health and Biomaterials, IBMM, Univ. Montpellier, CNRS, ENSCM, 34090 Montpellier, France;* orcid.org/0000-0002-8577-9273

Complete contact information is available at: https://pubs.acs.org/10.1021/acs.biomac.2c01408

Notes

The authors declare no competing financial interest.

■ ACKNOWLEDGMENTS

Campus France (PHC Van Gogh Project No. 44898RA "AeroMed") and the CNRS are gratefully acknowledged for funding. We thank Dr. Julien Jaxel (PERSEE, MINES Paris, France) for supercritical drying.

■ REFERENCES

(1) Muxika, A.; Etxabide, A.; Uranga, J.; Guerrero, P.; de la Caba, K. Chitosan as a Bioactive Polymer: Processing, Properties and Applications. *Int. J. Biol. Macromol.* **2017**, *105*, 1358−1368.

(2) Dash, M.; Chiellini, F.; Ottenbrite, R. M.; Chiellini, E. Chitosan—A Versatile Semi-Synthetic Polymer in Biomedical Applications. *Prog. Polym. Sci.* **2011**, *36*, 981−1014.

(3) Bernkop-Schnürch, A.; Dünnhaupt, S. Chitosan-Based Drug Delivery Systems. *Eur. J. Pharm. Biopharm.* **2012**, *81*, 463−469.
(4) Jiang, T.; James, R.; Kumbar, S. G.; Laurencin, C. T. Chitosan as a Biomaterial: Structure, Properties, and Applications in Tissue Engineering and Drug Delivery. *Natural and Synthetic Biomedical Polymers*; Elsevier, 2014; pp 91−113.
(5) Park, J.-U.; Song, E.-H.; Jeong, S.-H.; Song, J.; Kim, H.-E.; Kim, S. Chitosan-Based Dressing Materials for Problematic Wound Management. In *Novel Biomaterials for Regenerative Medicine*; Chun, H. J., Park, K., Kim, C.-H., Khang, G., Eds.; Springer: Singapore, 2018; Vol. *1077*, pp 527−537.
(6) Guebitz, G. M.; Pellis, A.; Nyanhongo, G. S. Delivery of Biomolecules Using Chitosan Wound Dressings. In *Chitosan for Biomaterials IV*; Jayakumar, R., Prabaharan, M., Eds.; Springer International Publishing, 2021; Vol. *288*, pp 447−467.
(7) López-Iglesias, C.; Barros, J.; Ardao, I.; Monteiro, F. J.; Alvarez-Lorenzo, C.; Gómez-Amoza, J. L.; García-González, C. A. Vancomycin-Loaded Chitosan Aerogel Particles for Chronic Wound Applications. *Carbohydr. Polym.* **2019**, *204*, 223−231.
(8) Buchtova, N.; Budtova, T. Cellulose Aero-, Cryo-and Xerogels: Towards Understanding of Morphology Control. *Cellulose* **2016**, *23*, 2585−2595.
(9) Groult, S.; Buwalda, S.; Budtova, T. Pectin Hydrogels, Aerogels, Cryogels and Xerogels: Influence of Drying on Structural and Release Properties. *Eur. Polym. J.* **2021**, *149*, 110386.
(10) Aegerter, M. A.; Leventis, N.; Koebel, M.; Steiner, S. A., III *Handbook of Aerogels*, 2nd ed.; Springer Nature: Switzerland, 2023.
(11) Zou, F.; Budtova, T. Tailoring the Morphology and Properties of Starch Aerogels and Cryogels via Starch Source and Process Parameter. *Carbohydr. Polym.* **2021**, *255*, 117344.
(12) Wang, X.; Li, X.; Stride, E.; Edirisinghe, M. Fabrication of Nanoporous Chitosan Membranes. *Nano* **2010**, *5*, 53−60.
(13) Álvarez-Suarez, A. S.; López-Maldonado, E. A.; Graeve, O. A.; Martinez-Pallares, F.; Gómez-Pineda, L. E.; Oropeza-Guzmán, M. T.; Iglesias, A. L.; Ng, T.; Serena-Gómez, E.; Villarreal-Gómez, L. J. Fabrication of Porous Polymeric Structures Using a Simple Sonication Technique for Tissue Engineering. *J. Polym. Eng.* **2017**, *37*, 943−951.
(14) Lim, J. I.; Lee, Y.-K.; Shin, J.-S.; Lim, K.-J. Preparation of Interconnected Porous Chitosan Scaffolds by Sodium Acetate Particulate Leaching. *J. Biomater. Sci. Polym. Ed.* **2011**, *22*, 1319−1329.
(15) Barroso, T.; Viveiros, R.; Casimiro, T.; Aguiar-Ricardo, A. Development of Dual-Responsive Chitosan−Collagen Scaffolds for Pulsatile Release of Bioactive Molecules. *J. Supercrit. Fluids* **2014**, *94*, 102−112.
(16) Alsmadi, M. M.; Obaidat, R. M.; Alnaief, M.; Albiss, B. A.; Hailat, N. Development, In Vitro Characterization, and In Vivo Toxicity Evaluation of Chitosan-Alginate Nanoporous Carriers Loaded with Cisplatin for Lung Cancer Treatment. *AAPS PharmSciTech* **2020**, *21*, 191.
(17) Wei, S.; Ching, Y. C.; Chuah, C. H. Synthesis of Chitosan Aerogels as Promising Carriers for Drug Delivery: A Review. *Carbohydr. Polym.* **2020**, *231*, 115744.
(18) Dragan, E. S.; Dinu, M. V. Advances in Porous Chitosan-Based Composite Hydrogels: Synthesis and Applications. *React. Funct. Polym.* **2020**, *146*, 104372.
(19) Chartier, C.; Buwalda, S.; Van Den Berghe, H.; Nottelet, B.; Budtova, T. Tuning the Properties of Porous Chitosan: Aerogels and Cryogels. *Int. J. Biol. Macromol.* **2022**, *202*, 215−223.
(20) Hao, H.; Wang, J.; Wang, Y. Solubility of Dexamethasone Sodium Phosphate in Different Solvents. *J. Chem. Eng. Data* **2004**, *49*, 1697−1698.
(21) Groult, S.; Budtova, T. Thermal Conductivity/Structure Correlations in Thermal Super-Insulating Pectin Aerogels. *Carbohydr. Polym.* **2018**, *196*, 73−81.
(22) Druel, L.; Bardl, R.; Vorwerg, W.; Budtova, T. Starch Aerogels: A Member of the Family of Thermal Superinsulating Materials. *Biomacromolecules* **2017**, *18*, 4232−4239.
(23) Gethin, G. The Significance of Surface PH in Chronic Wounds. *Wounds UK* **2007**, *3*, 52−56.
(24) Schneider, L. A.; Korber, A.; Grabbe, S.; Dissemond, J. Influence of pH on Wound-Healing: A New Perspective for Wound-Therapy? *Arch. Dermatol. Res.* **2007**, *298*, 413−420.
(25) Percival, S. L.; McCarty, S.; Hunt, J. A.; Woods, E. J. The Effects of pH on Wound Healing, Biofilms, and Antimicrobial Efficacy. *Wound Repair Regen.* **2014**, *22*, 174−186.
(26) Budtova, T. Cellulose II Aerogels: A Review. *Cellulose* **2019**, *26*, 81−121.
(27) García-González, C. A.; Jin, M.; Gerth, J.; Alvarez-Lorenzo, C.; Smirnova, I. Polysaccharide-Based Aerogel Microspheres for Oral Drug Delivery. *Carbohydr. Polym.* **2015**, *117*, 797−806.
(28) Groult, S.; Buwalda, S.; Budtova, T. Tuning Bio-Aerogel Properties for Controlling Theophylline Delivery. Part 1: Pectin Aerogels. *Mater. Sci. Eng., C* **2021**, *126*, 112148.
(29) Groult, S.; Buwalda, S.; Budtova, T. Tuning Bio-Aerogel Properties for Controlling Drug Delivery. Part 2: Cellulose-Pectin Composite Aerogels. *Biomater. Adv.* **2022**, *135*, 212732.
(30) Kumar, M. N. V. R.; Muzzarelli, R. A. A.; Muzzarelli, C.; Sashiwa, H.; Domb, A. J. Chitosan Chemistry and Pharmaceutical Perspectives. *Chem. Rev.* **2004**, *104*, 6017−6084.
(31) Behl, G.; Iqbal, J.; O'Reilly, N. J.; McLoughlin, P.; Fitzhenry, L. Synthesis and Characterization of Poly(2-Hydroxyethylmethacrylate) Contact Lenses Containing Chitosan Nanoparticles as an Ocular Delivery System for Dexamethasone Sodium Phosphate. *Pharm. Res.* **2016**, *33*, 1638−1648.
(32) Doustgani, A.; Farahani, E. V.; Imani, M.; Doulabi, A. H. Dexamethasone Sodium Phosphate Release from Chitosan Nanoparticles Prepared by Ionic Gelation Method. *J. Colloid Sci. Biotechnol.* **2012**, *1*, 42−50.
(33) Veronovski, A.; Tkalec, G.; Knez, Ž.; Novak, Z. Characterisation of Biodegradable Pectin Aerogels and Their Potential Use as Drug Carriers. *Carbohydr. Polym.* **2014**, *113*, 272−278.
(34) Mehling, T.; Smirnova, I.; Guenther, U.; Neubert, R. H. H. Polysaccharide-Based Aerogels as Drug Carriers. *J. Non-Cryst. Solids* **2009**, *355*, 2472−2479.
(35) Duarte, A. R. C.; Mano, J. F.; Reis, R. L. Preparation of Chitosan Scaffolds Loaded with Dexamethasone for Tissue Engineering Applications Using Supercritical Fluid Technology. *Eur. Polym. J.* **2009**, *45*, 141−148.
(36) Rojewska, A.; Karewicz, A.; Baster, M.; Zając, M.; Wolski, K.; Kępczyński, M.; Zapotoczny, S.; Szczubiałka, K.; Nowakowska, M. Dexamethasone-Containing Bioactive Dressing for Possible Application in Post-Operative Keloid Therapy. *Cellulose* **2019**, *26*, 1895−1908.
(37) Javed, Q. ul A.; Syed, M. A.; Arshad, R.; Rahdar, A.; Irfan, M.; Raza, S. A.; Shahnaz, G.; Hanif, S.; Díez-Pascual, A. M. Evaluation and Optimization of Prolonged Release Mucoadhesive Tablets of Dexamethasone for Wound Healing: In Vitro−In Vivo Profiling in Healthy Volunteers. *Pharmaceutics* **2022**, *14*, 807.
(38) Bhowmik, D.; Gopinath, H.; Kumar, B. P.; Duraivel, S.; Kumar, K. P. S. Controlled Release Drug Delivery Systems. *PHARMA Innov.* **2012**, *1*, 9.
(39) Siepmann, J.; Siepmann, F. Mathematical Modeling of Drug Delivery. *Int. J. Pharm.* **2008**, *364*, 328−343.
(40) Neto, A. S.; Pereira, P.; Fonseca, A. C.; Dias, C.; Almeida, M. C.; Barros, I.; Miranda, C. O.; de Almeida, L. P.; Morais, P. V.; Coelho, J. F. J.; Ferreira, J. M. F. Highly Porous Composite Scaffolds Endowed with Antibacterial Activity for Multifunctional Grafts in Bone Repair. *Polymers* **2021**, *13*, 4378.
(41) Uskoković, V. Mechanism of Formation Governs the Mechanism of Release of Antibiotics from Calcium Phosphate Nanopowders and Cements in a Drug-Dependent Manner. *J. Mater. Chem. B* **2019**, *7*, 3982−3992.

https://doi.org/10.1021/acs.biomac.2c01408
Biomacromolecules 2023, 24, 4494−4501